Lithos 260 (2016) 164–177

Contents lists available at ScienceDirect

Lithos

journal homepage: www.elsevier.com/locate/lithos

Cambrian intermediate-mafic magmatism along the Laurentian margin: Evidence for flood basalt volcanism from well cuttings in the Southern Oklahoma Aulacogen (U.S.A.)

Matthew E. Brueseke [a,*], Jasper M. Hobbs [a], Casey L. Bulen [a], Stanley A. Mertzman [b], Robert E. Puckett [c], J. Douglas Walker [d], Josh Feldman [d]

[a] Department of Geology, Kansas State University, 108 Thompson Hall, Manhattan, KS 66506, United States
[b] Earth and Environment, Franklin and Marshall College, P.O. Box 3003, Lancaster, PA 17604-3003, United States
[c] 12700 Arrowhead Lane, Oklahoma City, OK 73120, United States
[d] Department of Geology, University of Kansas, Lawrence, KS 66045, United States

ARTICLE INFO

Article history:
Received 24 February 2016
Accepted 28 May 2016
Available online 7 June 2016

Keywords:
Basalt
Large igneous province
Rifting
Iapetus
Southern Oklahoma Aulocogen
Cambrian

ABSTRACT

The Southern Oklahoma Aulocogen (SOA) stretches from southern Oklahoma through the Texas panhandle and into Colorado and New Mexico, and contains mafic through silicic magmatism related to the opening of the Iapetus Ocean during the early Cambrian. Cambrian magmatic products are best exposed in the Wichita Mountains (Oklahoma), where they have been extensively studied. However, their ultimate derivation is still somewhat contentious and centers on two very different models: SOA magmatism has been suggested to occur via [1] continental rifting (with or without mantle plume emplacement) or [2] transform-fault related magmatism (e.g., leaky strike–slip faults). Within the SOA, the subsurface in and adjacent to the Arbuckle Mountains in southern Oklahoma contains thick sequences of mafic to intermediate lavas, intrusive bodies, and phreatomagmatic deposits interlayered with thick, extensive rhyolite lavas, thin localized tuffs, and lesser silicic intrusive bodies. These materials were first described in the Arbuckle Mountains region by a 1982 drill test (Hamilton Brothers Turner Falls well) and the best available age constraints from SOA Arbuckle Mountains eruptive products are ~535 to 540 Ma. Well cuttings of the mafic through intermediate units were collected from that well and six others and samples from all but the Turner Falls and Morton wells are the focus of this study. Samples analyzed from the wells are dominantly subalkaline, tholeiitic, and range from basalt to andesite. Their overall bulk major and trace element chemistry, normative mineralogy, and Sr—Nd isotope ratios are similar to magmas erupted/emplaced in flood basalt provinces. When compared with intrusive mafic rocks that crop out in the Wichita Mountains, the SOA well cuttings are geochemically most similar to the Roosevelt Gabbros. New geochemical and isotope data presented in this study, when coupled with recent geophysical work in the SOA and the coeval relationship with rhyolites, indicates that the ~250,000 km^3 of early Cambrian mafic to silicic igneous rocks in the SOA were emplaced in a rifting event. This event is suggested to result from the break-up of Pannotia and the formation of the failed arm of a three-armed radial rift system.

1. Introduction

The Laurentian subcontinent was a component of two, Middle to Late Neoproterozoic supercontinents, Rodinia and Pannotia (or Greater Gondwanaland). Following the break-up of the Rodinia, North Rodinia and South Rodinia collided over a 100 Ma time period with the Congo craton to form the core of Pannotia (Scotese, 2009). The assembly of Pannotia repositioned Laurentia in the southeastern portion of the supercontinent. By the latest Precambrian (560 Ma), Pannotia was rifted into four separate continents and this rifting was accompanied by multiple episodes of intraplate magmatism along the eastern margin of the Laurentian craton (Central Iapetus Magmatic Province; Badger and Sinha, 1988; Badger et al., 2010; Ernst and Bleeker, 2010; McClellan and Gazel, 2014; Puffer, 2002; Youbi et al., 2011). The only evidence of early Cambrian magmatism along the southeastern Laurentian margin is in southern Oklahoma and northern Texas as part of the Southern Oklahoma Aulacogen (SOA; Hanson et al., 2013) (Figs. 1, 2). Early Cambrian rift volcanism is also reported from Morrocco (Álvaro et al., 2006; Pouclet et al., 2008) but reconstructions of Cambrian paleogeography don't show a spatial relationship between Morroccon magmatism and the magmatism discussed in this study (Dalziel,

* Corresponding author. Tel.: +1 785 532 1908; fax: +1 785 532 5159.
E-mail address: brueseke@ksu.edu (M.E. Brueseke).

http://dx.doi.org/10.1016/j.lithos.2016.05.016

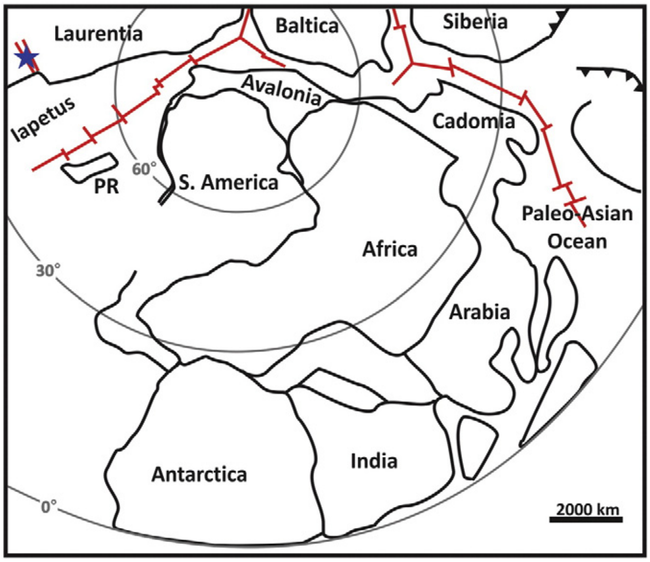

Fig. 1. Mid-Cambrian paleogeographic map after Thomas and Astini (1996), Golonka (2012), Golonka and Gaweda (2012), and Thomas et al. (2012). SOA is located with a blue star in upper-left of map. PR; Argentine Precordillera (For interpretation of the references to color in this figure legend, the reader is referred to the web version of this article.).

2014; Golonka and Gaweda, 2012; Fig. 1). For example, Thomas and Astini (1996) and Thomas et al. (2012) demonstrate that the Argentine PreCordillera was rifted away from Laurentia adjacent to the SOA (Fig. 1); it is difficult to reconcile this evidence while trying to directly link SOA magmatism to coeval activity in Morocco. The SOA contains extensive igneous rocks that are exposed in the Wichita Mountains and encountered mostly in the subsurface near the Arbuckle Mountains of southern Oklahoma (Fig. 2). These exposures represent the largest magmatic episode related to the opening of the Iapetus Ocean and the break-up of Pannotia, thus warrant study to shed light on how this particular Wilson Cycle evolved.

The SOA extends from northeastern Texas through southern Oklahoma, northwestern Texas, and likely across parts of New Mexico and Colorado (Fig. 2). A minimum of 250,000 km^3 of compositionally bimodal silicic-mafic magma was emplaced or erupted in the aulacogen (Hanson et al., 2013). Most workers consider the SOA a failed third arm of a triple junction rift system (Hanson et al., 2013). Bounding fault geometry and seismic profiles indicate a rift up to 150 km wide with emplaced/erupted igneous rocks and sedimentary rift fill as thick as 15 km (Hanson et al., 2013; Keller and Stephenson, 2007). Initially, mafic magmatism was thought to be mostly restricted to the emplacement of voluminous layered gabbros in the Wichita Mountains area prior to felsic magmatism. Minor amounts of basalt were known only in scattered subsurface-drilled sections and from outcrops of sills and dikes cutting felsic rocks. Drilling through overthrust sections of rift-related igneous rocks in the Arbuckle Mountains area of southern Oklahoma and recent geological mapping has now documented a much more extensive suite of erupted mafic and intermediate lava packages and phreatomagatic deposits intercalated with rhyolite lavas, which are likely analogous to the Navajoe Mountain Basalt-Spilite Group described in the Wichita Mountains region subsurface

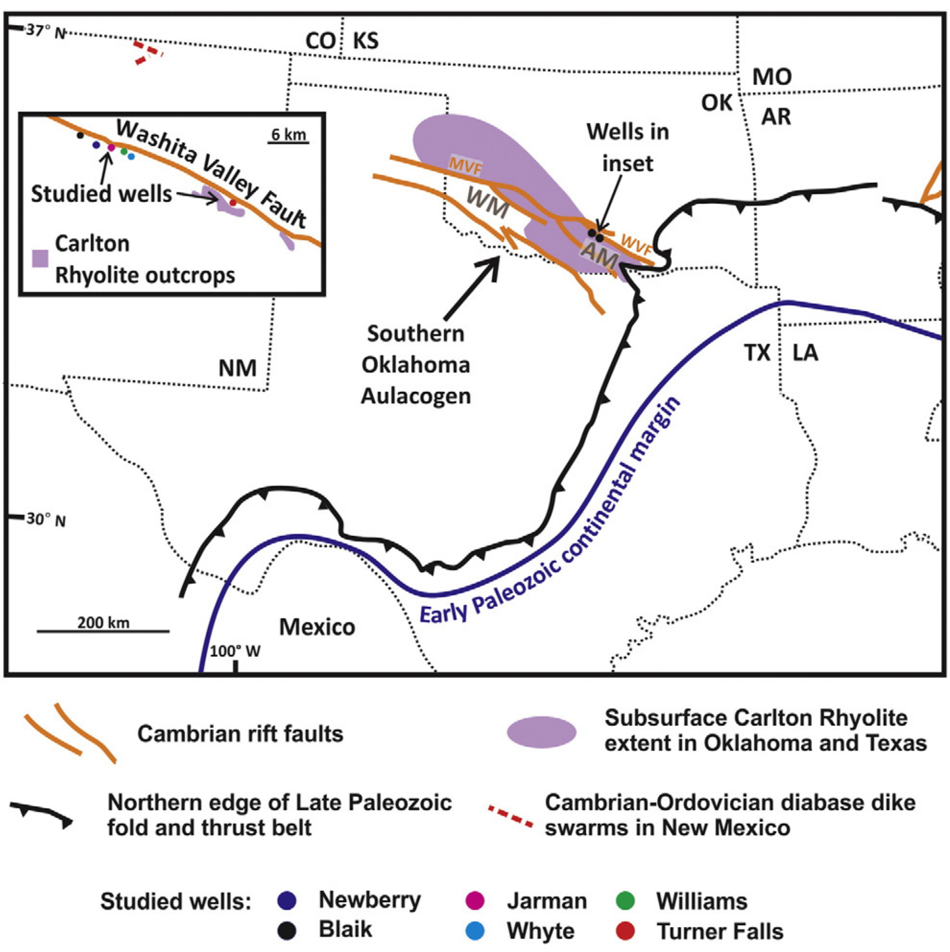

Fig. 2. Map of Southern Oklahoma aulacogen (after Hanson et al., 2013). Major tectonic features and Cambrian rhyolite extent in the SOA are indicted. The inset displays the six wells in this study and the Mill Creek Dike location is approximately at the "t" in the word "fault." CO: Colorado; OK: Oklahoma; MO: Missouri; AR; Arkansas; LA: Louisiana; TX: Texas; NM: New Mexico; WM: Wichita Mountains, AM; Arbuckle Mountains; WVF: Washita Valley Fault.

(Ham et al., 1964). The Navajoe Mountain Basalt-Spilite Group is a package of basaltic to intermediate volcanic rocks, including phreatomagmatic deposits and lavas, intersected by drilled wells (Ham et al., 1964). Shapiro (1981) and Aquilar (1988) were the last to study the geochemistry of these rocks, and analyzed a subset of samples for select major and trace element compositions and reported tholeiitic compositions.

In the Wichita Mountains west of our study area (Fig. 2), mafic plutons equivalent to hydrous olivine tholeiites are known as the Roosevelt Gabbros. These magmas intruded through the earlier Glen Mountains Layered Complex (GMLC), a series of anhydrous alumina-rich layered gabbros that are interpreted to have crystallized from a tholeiitic parental magma (Cameron et al., 1986; McConnell and Gilbert, 1990). The Roosevelt Gabbros have been dated via $^{40}Ar/^{39}Ar$ geochronology from hornblende and biotite, at 533 ± 2 and 533 ± 4 Ma, respectively (Hames et al., 1998). The GMLC is a 3 to 5-km-thick layered complex that extends for over 1000 km^2 and yields a Sm—Nd isochron date of 528 ± 29 Ma (Lambert et al., 1988). Other U—Pb ages of Wichita area intrusive mafic rocks range from 577 ± 2 Ma to 552 ± 7 Ma, while the U—Pb in zircon ages of felsic rocks (rhyolite lavas and granitoid intrusions) cluster around 530 to 535 Ma (Bowring and Hoppe, 1982; Degeller et al., 1996; Hanson et al., 2009; Hogan and Amato, 2015; Wright et al., 1996). No gabbros have been encountered on the surface or in the subsurface in the Arbuckle Mountains area. In the Wichita Mountains, following a period of erosion and gentle tilting, extensive rhyolite lavas erupted from fissure vents onto the weathered gabbro surface (Hanson et al., 2014). Tabular granite bodies, known as the Wichita Granite Group (Keller and Stephenson, 2007) were later injected into the contact between the gabbros and the overlying rhyolites. The silicic magmas, comprising both the rhyolites and granites, likely formed from fractional crystallization of a large body of basaltic magma underlying the SOA, as well as by partial melting of crust (Hanson and Al-Shaieb, 1980; Hanson et al., 2013, 2014).

The igneous history of the SOA in the Arbuckle Mountains is less well understood, primarily due to the paucity of surface exposures of Cambrian igneous rocks; where present, they are limited to rhyolite lavas and pyroclastic deposits similar to those in the Wichita Mountains and mafic phreatomagmatic vent complexes and deposits (Eschberger et al., 2014; Hanson and Eschberger, 2014; Hanson et al., 2013; Toews et al., 2015). Outcrop studies of the rhyolites indicate voluminous emplacement at high temperatures, similar to rhyolites documented elsewhere associated with flood basalt volcanism (e.g., the Oregon Plateau, U.S.A.; Manley, 1996; the Snake River plain; Branney et al., 2008; Karoo large igneous province; Milner et al., 1992; Keweeenawan rift; Green and Fitz, 1993). The complete interval of rift related igneous rocks in the Arbuckle area has never been penetrated making reconstruction of the sequence of igneous activity impossible. The major mafic-intermediate lavas found in the subsurface are intercalated with mafic phreatomagmatic deposits and sedimentary strata, and are intruded by epizonal granites and diabase sills (Hanson et al., 2014; Puckett et al., 2014; Toews et al., 2015) (Fig. 3). These rocks are believed to be early Cambrian in age based on U—Pb dating of zircons from exposed Carlton Rhyolite Group eruptive units in the Arbuckle Mountains (539 ± 5 Ma and 536 ± 5 Ma, Hanson et al., 2013; Thomas et al., 2012) and are the subject of this study. Following the cessation of volcanism, the SOA underwent a period of quiescence, followed by rapid subsidence and accumulation of a thick sequence of Paleozoic rocks. In the late Pennsylvanian, the aulacogen was tectonically inverted, re-activating the bounding normal faults as regional transpressive thrust faults (Hoffman et al., 1974). The thickest accumulation of mafic lavas in the Arbuckle Mountains study areas was described in the Hamilton Brothers Oil Co. #1–18 Turner Falls well (drilled 1980–81), which penetrated 4.82 km of Cambrian rift-related igneous rock including a cumulative total of 2.74 km of basalt with minor amounts of diabase (Puckett et al., 2014). Evidence of mafic-intermediate lavas in this area has now been documented in 21-drilled wells drilled from the 1950s to 2001 for which drill cuttings are available.

Thomas (2006, 2014) suggested that the intersection of both the SOA and the Alabama–Oklahoma transform fault with the Ouachita thrust system is evidence that the SOA formed as a leaky transform fault system, which, according to those studies, correlates with a bend in the Grenville front and also matches up with Precambrian mafic dikes found in the Arbuckle Mountains. Conversely, large igneous provinces (LIPs) are defined by a large volume of magmatism produced over a relatively short period of time (Bryan and Ernst, 2008) and can form from purely upper-mantle processes (e.g., continental rifting) or processes that involve a component of lower mantle upwelling (e.g., a mantle plume) that forces continental rifting. Flood basalt volcanism is a component of many LIPs and these mafic eruptions represent the largest on Earth (Bryan and Ferrari, 2013). Typically, most flood basalt eruptions occur from numerous polygenetic and monogenetic vents, leading to extensive and voluminous packages of mafic lavas (Sheth and Cañón-Tapia, 2014; Walker, 1993), as well as interspersed rhyolites, minor intermediate lavas, and sedimentary strata. Interpreting the SOA as a large igneous province (LIP) is more consistent with the volume of extrusive lavas mapped on the surface and inferred to exist in the subsurface based on geophysical studies (Hanson et al., 2013; Keller and Stephenson, 2007).

The geochemical and isotope characteristics of the well cuttings can be used to decipher whether their origin is consistent with rifting and continental break-up. Also, as with all dominantly mafic lavas, geochemistry will give insight into defining potential mantle sources involved in magmatism, and deciphering these sources is a key to understanding more about magma genesis in the SOA. By providing new geochemical and Sr-Nd radiogenic isotope data, this study provides new insights into the petrologic constraints and tectonic implications of SOA mafic volcanism that affected the southern Laurentian margin in the Cambrian.

2. Methods

Studying well cuttings is useful in situations where no equivalent surficial rock outcrops exist and core sampling did not occur (Arce et al., 2013). While there is obvious uncertainty in working with cuttings, they provide the only accessible information about the thick volcanic package in the SOA. The subject wells were drilled with fresh-water based neutral-ph drilling fluids and samples were collected at 3 m intervals. Screening is used to concentrate the size of cuttings produced by the drill bit versus larger cavings from previously penetrated intervals. Thus, potential contamination by younger material was minimal (see below), the specific sample depth of each set of cuttings is known (Fig. 3 and Appendix A), and drilling fluid contamination was not an issue.

All samples were collected from the Oklahoma Geological Survey sample library at the Oklahoma Petroleum Information Center in Norman, Oklahoma. These wells were chosen for the thickness of the mafic packages based on logging, and the depths from which the samples were picked were chosen based on the amount of sample, size of the cuttings, and the amount of mafic material visible under binocular microscope. We did not sample any felsic material, though felsic rocks and sedimentary strata are interspersed within the sampled stratigraphy (Fig. 3). Where available, sensitivity of the produced cuttings to lithologic changes was confirmed by correlation to well logs (Fig. 3; Puckett et al., 2014). In total, 40 new samples of well cuttings were collected from three wells in the Western Arbuckle Mountains region: Pan-Am Whyte Unit #1, Blaik Oil Co. #1 and B-13 Morton. On further inspection, the Morton cuttings were too small to effectively work with and ensure sample homogeneity and lack of post-emplacement alteration, thus they were not processed further. Thus 28 new samples were combined with an existing dataset of 47 cuttings from three wells (Brueseke et al., 2014; Bulen, 2012) to yield

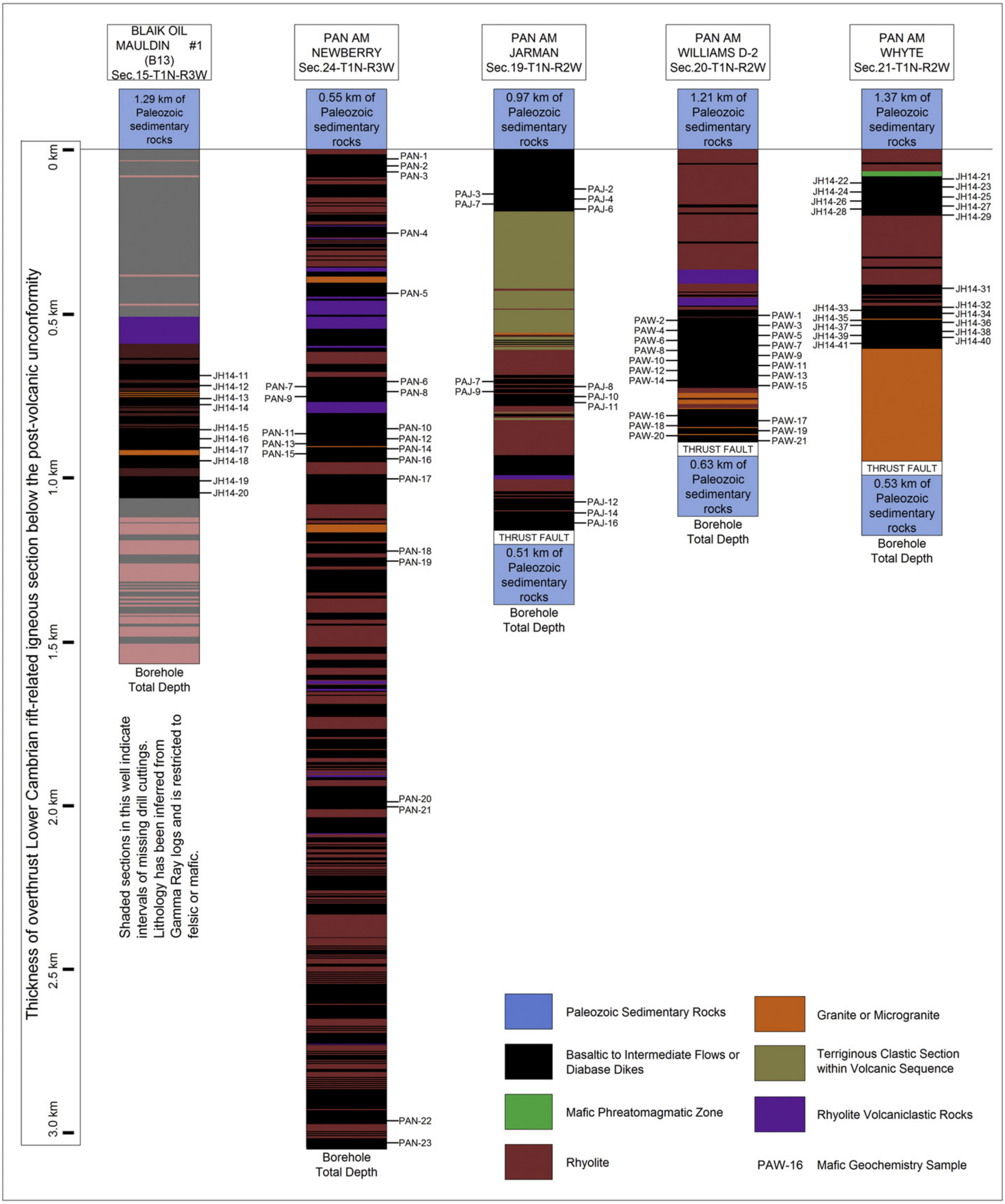

Fig. 3. Well stratigraphy (after Puckett et al., 2014). Notice rhyolite lavas, sedimentary and volcaniclastic strata, and mafic phreatomagmatic deposits that are interlayered with the sampled rocks. The fault at the base of most sections is the Washita Valley Fault; fault was not intersected in the Blaik or Newberry wells.

a suite of 76 total samples from five wells. Average sample depths for each well are listed in Appendix A (Supplementary Data) and illustrated in Fig. 3.

All samples were handpicked at Kansas State University using a binocular microscope to remove any mineral fragments, foreign rocks, and/or obviously altered rock cuttings, with the goal of ensuring that only petrographically homogeneous rock fragments remained for further crushing. After handpicking, samples containing more than 8 g of cuttings were crushed (<200 mesh-sieve size) in a Spex Industries aluminum oxide shatterbox.

Samples were sent to Franklin and Marshall College for XRF analysis of major and trace element compositions and loss on ignition (LOI) following the method outlined in Mertzman (2000, 2015) and online at http://www.fandm.edu/earth-environment/laboratory-facilities/instrument-use-and-instructions. One-gram of powder from each sample was placed in clean ceramic crucibles and heated at 900 °C in a muffle furnace for 60–75 min. After cooling to room temperature, samples were reweighed and the change in percent was reported as loss on ignition (LOI). Following LOI determinations, 0.4 g of anhydrous powder was mixed with 3.6 g of lithium tetraborate ($Li_2B_4O_7$) and melted in 95% Pt − 5% Au crucibles. Once quenched into homogeneous glass disks, the disks were used for XRF analysis of major elements using a Panalytical, Inc. 2404 XRF vacuum spectrometer equipped with a 4 kW Rh X-ray tube. Major elements reported as weight percent oxide (SiO_2, Al_2O_3, CaO, K_2O, P_2O_5, TiO_2, Fe_2O_3, MnO, Na_2O, and MgO). Nineteen trace elements (Rb, Sr, Y, Zr, Nb, Ni, Ga, Cu, Zn, U, Th, Co, Pb, Sc, Cr, V, La, Ce, and Ba) were analyzed on pressed powder briquettes made from a mixture of 7.0 g of whole-rock sample powder and 1.4 g of high purity Copolywax powder. Trace element concentrations are presented as parts per million (ppm). Iron was corrected following LeMaitre (1976) and all data presented here in diagrams is recalculated on an anhydrous basis.

Rare earth element (REE) analyses were performed at Miami University (Ohio) by ICP-MS. Ten samples were selected, including the seven samples analyzed for Sr—Nd isotope compositions, as a representative subset of the entire suite (Table 1). About 75 mg of a 3:2 mixture of sodium tetraborate and potassium carbonate was used as a flux and mixed with 50 mg of sample powder. This mixture was heated at 950 °C for 30 min in a graphite crucible. After cooling, the mixture was moved to an acid-washed, polyethylene bottle, containing 125 ml

Table 1
Representative geochemical and isotopic data for SOA well cuttings.

Well	Blaik	Blaik	Whyte	Williams	Williams	Williams	Newberry	Newberry	Newberry	Jarman	Jarman
Sample	JH14–12	JH14–16	JH14–40	CB-PAW-19	CB-PAW-14	CB-PAW-1	CB-PAN-8	CB-PAN-16	CB-PAN-20	CB-PAJ-10	CB-PAJ-13
SiO2	57.53	50.32	55.65	53.74	54.99	50.03	53.45	60.00	46.17	57.02	54.94
TiO2	2.58	3.13	1.65	2.10	2.15	2.50	2.63	2.18	2.90	1.73	1.67
Al2O3	12.70	13.29	13.26	13.24	12.69	14.24	13.40	13.04	14.52	13.40	13.24
Fe2O3	11.99	15.02	12.84	14.18	15.02	13.67	13.30	10.12	15.26	12.38	13.16
MnO	0.19	0.29	0.20	0.23	0.23	0.26	0.20	0.18	0.23	0.16	0.20
MgO	3.22	5.37	3.56	4.33	3.04	6.23	4.17	2.19	6.38	4.12	4.26
CaO	5.07	6.49	6.61	6.42	5.75	7.67	6.85	5.19	10.37	5.33	6.66
Na2O	3.42	3.74	4.22	3.59	3.33	3.63	3.17	3.40	2.52	2.68	3.47
K2O	2.33	1.48	1.52	1.74	2.55	1.39	1.70	2.80	0.75	2.19	1.92
P2O5	0.37	0.46	0.33	0.37	0.42	0.37	0.41	0.63	0.38	0.32	0.30
Total	99.40	99.59	99.84	99.94	100.17	99.99	99.28	99.73	99.48	99.33	99.82
LOI	2.55	2.84	1.15	2.64	1.13	3.66	2.50	1.88	2.44	6.10	2.31
Rb	48	30	25	32	25	25	28	52	13	38	29
Sr	290	328	232	262	330	382	328	370	438	218	292
Y	50	38	49	42	46	31	42	56	25	48	41
Zr	400	217	299	226	240	149	284	431	119	293	206
V	240	305	282	284	278	340	298	137	372	260	288
Ni	31	59	36	38	24	69	48	16	75	41	39
Cr	53	85	45	58	21	121	89	17	111	42	45
Nb	39	27	31	27	25	21	29	42	16	36	22
Ga	20	18	19	17	17	15	19	20	17	17	15
Cu	117	158	159	109	106	111	132	34	87	103	95
Zn	156	139	131	151	131	122	127	126	109	110	105
Co	39	56	46	48	48	51	43	25	56	44	45
Ba	501	481	464	378	411	338	425	639	346	370	419
U	0.8	0.9	<0.5	0.9	<0.5	<0.5	1.2	2.8	1.1	1.8	1.4
Th	4.8	1.1	6.2	11	9.7	4.3	4.2	6.7	4.4	7.1	2.5
Sc	24	30	30	34	36	36	29	21	40	31	33
Pb	10	<1	<1	10	<1	14	1.0	<1	3.0	<1	<1
La	40.1	25.2	31.3	30.3	21	19.4	33.1	51.2	15.6	33.8	26.0
Ce	91.1	59.3	69.6	70.1	46	44.6	76.1	116.9	36.2	77.0	58.7
Pr	11.2	8.4	8.8	9.1		6.7	9.5	14.5	5.5	9.0	7.9
Nd	49.4	40.4	39.8	44.7		29.6	46.2	61.7	25.4	40.4	34.1
Sm	11.3	9.4	6.9	10.2		6.6	9.6	15.7	5.9	6.9	6.2
Eu	2.6	2.8	1.8	2.8		2.2	2.5	3.8	2.2	1.6	1.7
Gd	11.7	9.3	7.9	10.4		6.5	10.0	15.5	6.2	7.7	7.0
Tb	1.9	1.5	1.5	1.7		1.0	1.7	2.4	1.0	1.4	1.2
Dy	11.1	8.3	9.0	9.8		5.9	9.5	13.7	5.6	8.8	7.5
Ho	2.2	1.6	1.9	2.0		1.2	1.9	2.7	1.1	1.8	1.5
Er	6.2	4.5	5.4	5.7		3.3	5.3	7.5	3.0	5.3	4.5
Tm	0.9	0.6	0.8	0.8		0.5	0.7	1.0	0.4	0.8	0.6
Yb	5.6	3.9	5.0	5.1		3.0	4.6	6.5	2.6	4.9	4.2
Lu	0.8	0.6	0.7	0.8		0.4	0.7	0.9	0.4	0.7	0.6
$^{87}Sr/^{86}Sr_m$					0.70685	0.70669	0.70643	0.70799	0.70459	0.71007	0.70703
$^{87}Sr/^{86}Sr_i$					0.70638	0.70564	0.70464	0.70776	0.70319	0.70877	0.66693
$^{143}Nd/^{144}Nd_m$					0.51251	0.51259		0.51249	0.51265	0.51253	0.51257
epsilon Nd_i					1.9	3.5		2.2	4.1	2.9	3.4

Notes: Major element concentrations are reported as weight percent oxides and expressed as raw data; trace element concentrations are reported in ppm. Major element analyses were analyzed by XRF (X-ray fluoresence) at Franklin and Marshall College. Miami University. All trace elements were analyzed by XRF at Franklin and Marshall College with the following exception: samples with rare earth data, where all REE results are ICP-MS (inductively coupled plasma mass spectrometry) data run at Miami University. All isotopic data was obtained by TIMS (thermal ionization mass spectrometry) at the Univ. of Kansas and reported to 535 Ma.

of 1% HNO_3. The samples were allowed to dissolve overnight. Following dissolution, samples were then analyzed using a Varian "Red Top" ICP-MS. The ICP-MS was calibrated and internal standardization utilized a 100 ppb solution of Ge, Re, Bi, and In. For each sample, three runs of 30 readings were completed.

Whole rock Sr and Nd isotope analyses were performed by TIMS at the University of Kansas on a subset of seven samples previously analyzed for bulk rock geochemistry by Bulen (2012) (Table 1). Samples were prepped for analysis by using standard HF-HNO_3 and HCl dissolution techniques. Elemental separation was done using ion exchange columns. Sr was isolated and collected using cation exchange columns with Biorad resin. Nd and Sm were purified using Eichrome LN spec resin columns. Samples were analyzed following the procedures of Krogh (1982), and Patchett and Ruiz (1987), details may be found at https://geo.ku.edu/tims-details. Analyses for Sr and Nd were completed on a VG Sector 54, with internal and external precisions of ± 20 ppm. After correcting for fractionation using $^{86}Sr/^{88}Sr = 0.1194$, Sr ratios are referenced to a value of 0.710250 for the $^{87}Sr/^{86}Sr$ ratio of NBS987. The measured laboratory value was 0.710247 on NBS987 over a 53 run period of analysis. Nd ratios were corrected using an internal standard tied to a value of 0.511860 for $^{143}Nd/^{144}Nd$ for LaJolla Nd. Fractionation was corrected using a $^{146}Nd/^{144}Nd$ ratio of 0.7219. Initial Sr and Nd isotope ratios are reported age-corrected to 535 Ma (Table 1). Given the wide spread of ages reported from SOA rocks, this age represents a minimum age for SOA magmatism and is consistent with the ~535 to 540 Ma ages reported for local Arbuckle Mountains area rhyolite volcanism (Thomas et al., 2012).

Some samples showed signs of alteration. Puckett (2011) reported that the samples found in the Turner Falls well were partially altered through multiple processes including carbonate replacement of plagioclase, chloritization of matrix minerals, and epidotization of mafic minerals. Although cuttings that showed obvious alteration were removed during the cleaning and preparation phase, it is possible that the results were still affected by alteration. To rule out potential alteration effects on the geochemistry of these samples, an "alteration filter", proposed by Beswick and Soucie (1978), was applied. This "alteration filter" plots molecular proportions of major element ratios (Al_2O_3/K_2O, SiO_2/K_2O, CaO/K_2O, etc.) on a logarithmic XY-plot (Beswick and Soucie, 1978). Unaltered samples will appear clustered in linear array on these plots whereas any significant variation from the linear array is suggestive of post-eruptive. Two samples (JH-14-21, JH-14-22) did not fall along the linear array on multiple plots that used the alteration filter and both of these samples have been removed from consideration in this study (Hobbs, 2015). Bulen (2012) took an identical approach for the cuttings from the other wells we discuss here.

3. Results

This study provides new major and trace element data from 28 samples, which we combine with major and trace element results (and new REE and Sr—Nd isotope data) from samples previously studied by Bulen (2012) and Brueseke et al. (2014) to yield a combined dataset of 76 samples. The samples analyzed by Bulen (2012) and discussed in Brueseke et al. (2014) come from three wells within the SOA that are located along strike, northwest of the Turner Falls well and southeast of the Blaik and Whyte wells (Figs. 2, 3). A complete list of samples and geochemical/isotope results are in Appendix A. Representative geochemical analyses and all Sr-Nd isotope analyses are presented in Table 1.

3.1. Petrography

The cuttings produced by the drilling process are generally less than 5 mm in any dimension. Under stereoscopic microscope examination, basalt is not distinguishable from andesitic composition, however samples display differences in crystallinity and in some cases <1 mm plagioclase is present. Carbonate alteration is discernable by anomalous light gray color; most of the cuttings are dark gray to black. In thin section, plagioclase is the dominant phenocryst, frequently altered to sericite, epidote, prehenite, and carbonate (Puckett et al., 2014). Mafic silicate phenocrysts (olivine and pyroxene as indicated by pseudomorph shapes) have been mostly replaced by green clay. Groundmass minerals include Fe-Ti oxides, plagioclase, olivine, and clinopyroxene (Puckett et al., 2014). Scattered flow-aligned amygdules up to 1.5 mm long are present, filled by secondary minerals. A wide range of groundmass textures are observed including quench, intergranular (plagioclase microlites with clinopyroxene), and intersertal (altered glass separating plagioclase microlites) textures. These textures are typical of subaerial basalt lavas and vary with position in the lava and contact with ground water (phreatomagmatic eruption) or flow into shallow lakes (Puckett et al., 2014).

3.2. Geochemical classification

On the total alkalis versus silica (TAS) diagram of LeBas et al. (1986), the new samples plot as subalkaline to transitional (trachy-)basalts to (trachy-)andesites, with SiO_2 values ranging from 47.6 to 61.2 wt.% (Fig. 4). The samples lie along a positive linear array with increasing alkali contents as silica content increases. New data partially overlap with existing data from the Newberry, Jarman, and Williams wells (Fig. 4). The entire Arbuckle suite we sampled ranges from basalt to andesite (Fig. 4). The well cuttings also plot as subalkaline to transitional on the Zr/TiO_2 versus Nb/Y diagram of Winchester and Floyd (1977) (Fig. 4). That the samples yield the same results on both classification schemes is significant and indicates that any alteration has had minimal effect on the behavior of incompatible trace elements and their overall bulk chemistry.

CIPW normative compositions of our samples plot as either olivine or quartz tholeiites on the expanded basalt tetrahedron of Thompson et al. (1983) (Fig. 5). Most samples scatter near the projection of the experimental 1 atm olivine + plagioclase + clinopyroxene + liquid cotectic toward normative quartz. However, a group of seven samples (JH14–23 to 29) from the Whyte well are closer to the higher-pressure plagioclase + clinopyroxene ± olivine ± magnetite + tholeiitic andesite liquid cotectic, possibly suggesting a different, deeper, differentiation history. These samples are also from a stratigraphically higher location in the Whyte well (Fig. 3) and as illustrated in Figs. 6 and 7, have lower wt.% CaO and ppm Sr than other rocks in this study, at a given wt.% SiO_2.

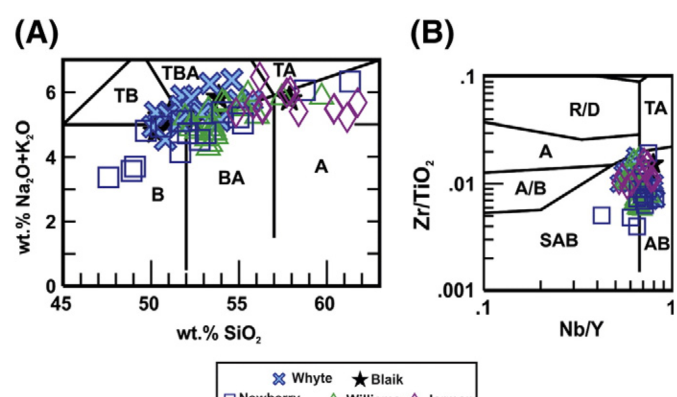

Fig. 4. (A) Volcanic rock classification based on total alkalies vs. silica (LeBas et al., 1986). (B) Discrimination diagram of Winchester and Floyd (1977). R/D: rhyodacite/dacite; TA: trachyandesite; A: andesite; A/B: andesite/basalt; SAB: subalkaline basalt; AB: alkaline basalt; TB: trachybasalt; BTA: basaltic trachyandesite; B: basalt; BA: basaltic andesite.

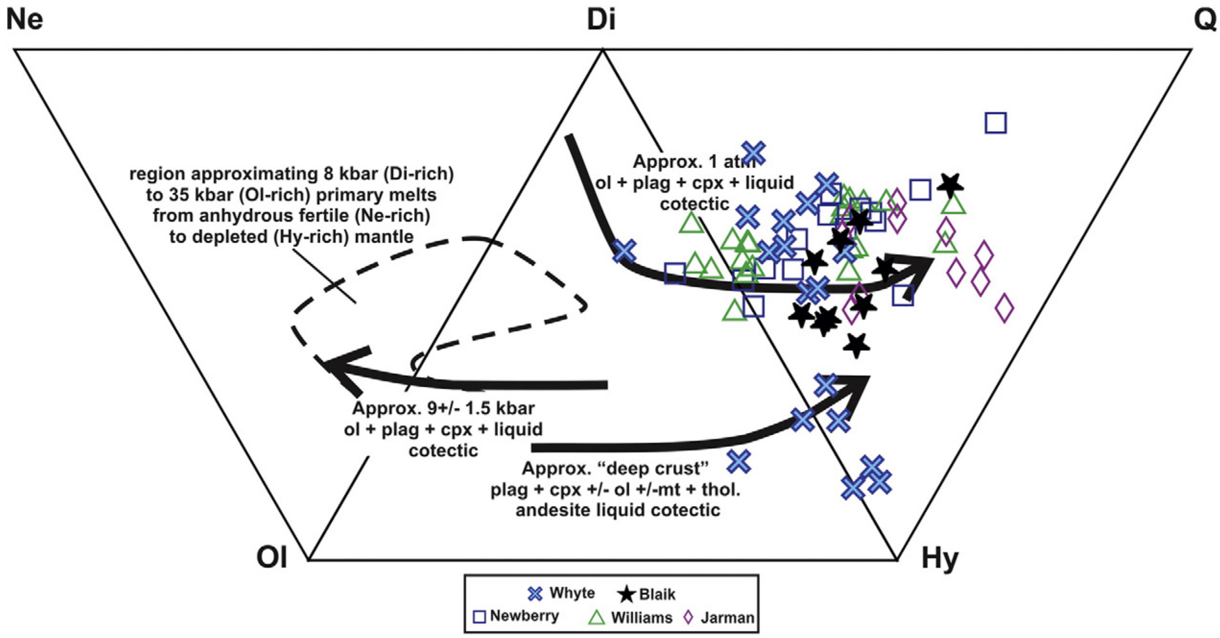

Fig. 5. Expanded basalt tetrahedron of Thompson et al. (1983). Most analyzed basalt-andesite samples from the Arbuckle Mountains plot near the 1 atm cotectic, except for a subset of samples from the Whyte well which plot closer to the deep crust cotectic (Thompson et al., 1983).

3.3. Major and trace element geochemical characteristics

The rocks are characterized by SiO_2 ranging from 47 to 62 wt.% and MgO values from 2.0 to 7.1 wt.% (Mg#, defined as [100 MgO/(MgO + FeO)] in mole %, = 29 to 50) (Fig. 6). As wt.% SiO_2 increases, so do wt.% Na_2O and K_2O and wt.% MgO, CaO, FeO and Fe_2O_3 decrease. TiO_2 concentrations range from 1.7 to 3.9 wt.% and high (TiO_2 > 2.5 wt.%) and low wt. % TiO_2 groups are present. Samples with high wt.% TiO_2 (Newberry, Blaik, and some Jarman samples) also have higher wt.% P_2O_5 concentrations at a given silica concentration. Furthermore, it is apparent that some samples cluster together on these diagrams (e.g., high wt.% FeO* [total Fe expressed as FeO] Newberry samples, high wt.% TiO_2 Newberry and Blaik, high wt.% MgO Whyte and Williams) this may reflect the occurrence of separate magma batches in the eruptive systems that are recorded in/across multiple wells. Sample suites from individual wells also show coherent patterns; for example differentiation arrays (e.g., increasing wt.% SiO_2 and decreasing wt.% MgO, FeO*, TiO_2, CaO, Na_2O, P_2O_5, and increasing wt.% K_2O) appear to exist among samples in most wells. Lidiak et al. (2014) demonstrated that Cambrian diabase dikes that are found just east of our study area are characterized by high FeO*/MgO and are high-Fe tholeiites. Our samples have overlapping FeO*/MgO ratios and support the assertion of Lidiak et al. (2014) that the dikes likely represent feeders for a synmagmatic LIP (e.g., the cuttings are from the erupted lavas).

Trace element concentrations (in ppm) are plotted against wt.% SiO_2 in Fig. 7. Sample concentrations decrease in Sr, Ni, Y, and Sc, and they increase in Zr, La, Nb, and Ba with increasing wt.% SiO_2. Overall, samples from individual wells generally overlap with each other. A primitive mantle-normalized multi-element diagram (Fig. 8) shows that the suite of samples has broadly the same overall enrichments and depletions (e.g., LILE enrichment, negative Sr anomaly) though variability is present. For example, Newberry samples are among both the most enriched and most depleted compositions. The overall patterns show that the rocks are more enriched than mid-ocean ridge basalts and instead resemble ocean-island basalts (Fig. 8). Fig. 9 illustrates that most samples have similar enrichment in light rare earth elements (LREE) compared to the heavy rare earth elements (HREE), are characterized by negative Eu anomalies consistent with plagioclase fractionation, and have flat HREE patterns. However, CB-PAW-1 (Williams) and CB-PAN-20 (Jarman) have slightly positive or no Eu anomalies; this coupled with their higher (relative to other samples) Sr concentrations, may reflect plagioclase accumulation (CB-PAW-1) or lack of plagioclase fractionation (CB-PAN-20).

Bulen (2012) and Hobbs (2015) observed within-well geochemical changes as a function of sampling depth and suggested this is due to the presence of distinct lava (flow) packages sampled by the drilling. For example, in the Whyte well, there is a gap of ~200 m between JH14–29 and JH14–31 which separates samples into a shallow group (samples JH-1423 through JH-1429) and a deep group (samples JH14–31 through JH14–41) (Fig. 3). The shallow group samples tend to have similar geochemical traits, while the deeper samples show ranges (Fig. 10). The shallow Whyte cluster overlaps with the least evolved compositions observed for the deep cluster: Zr between 175 and 225 ppm, Ni between 60 and 75 ppm, La between 12 and 18 ppm and SiO_2 between 50 and 52 wt.% (Fig. 10). In the deep group, wt.% SiO_2 decreases with ascending depth, while Ni, FeO*, and MgO increase while incompatible elements (e.g., Zr, La) decrease in concentration (Fig. 10). This kind of variation (e.g., less-evolved toward the surface) may represent the tapping + eruption of an evolving magma body that was (re)-filling with more primitive magma through time and is consistent with the type of recharge and crystallization scenarios observed in mafic layered intrusions and areas of voluminous mafic volcanism (Shervais et al., 2006). As mentioned, similar variations, both at the scale of specific depth ranges in individual SOA wells, and throughout the entire mafic-intermediate stratigraphy encountered by wells, indicates that the wells intersected different lava packages. TiO_2 vs. P_2O_5 differences have been used in other flood basalt provinces to distinguish between individual lavas and packages (Hooper, 2000) and these variations for the cuttings are in Fig. 11. It is apparent that Newberry and Blaik samples overlap in wt.% TiO_2 vs. P_2O_5 space; both wells are adjacent to each other (Fig. 2) and most of the Newberry samples are stratigraphically equivalent to the Blaik samples (Fig. 3). These samples also plot in similar positions in the Harker diagrams depicted in Figs. 6 and 7. Thus, it is likely that both wells intersected the same lava package, which is continuous across a portion of the SOA as expected in a flood basalt province. The chemostratigraphic variations also illustrate that while the wells are located in close proximity

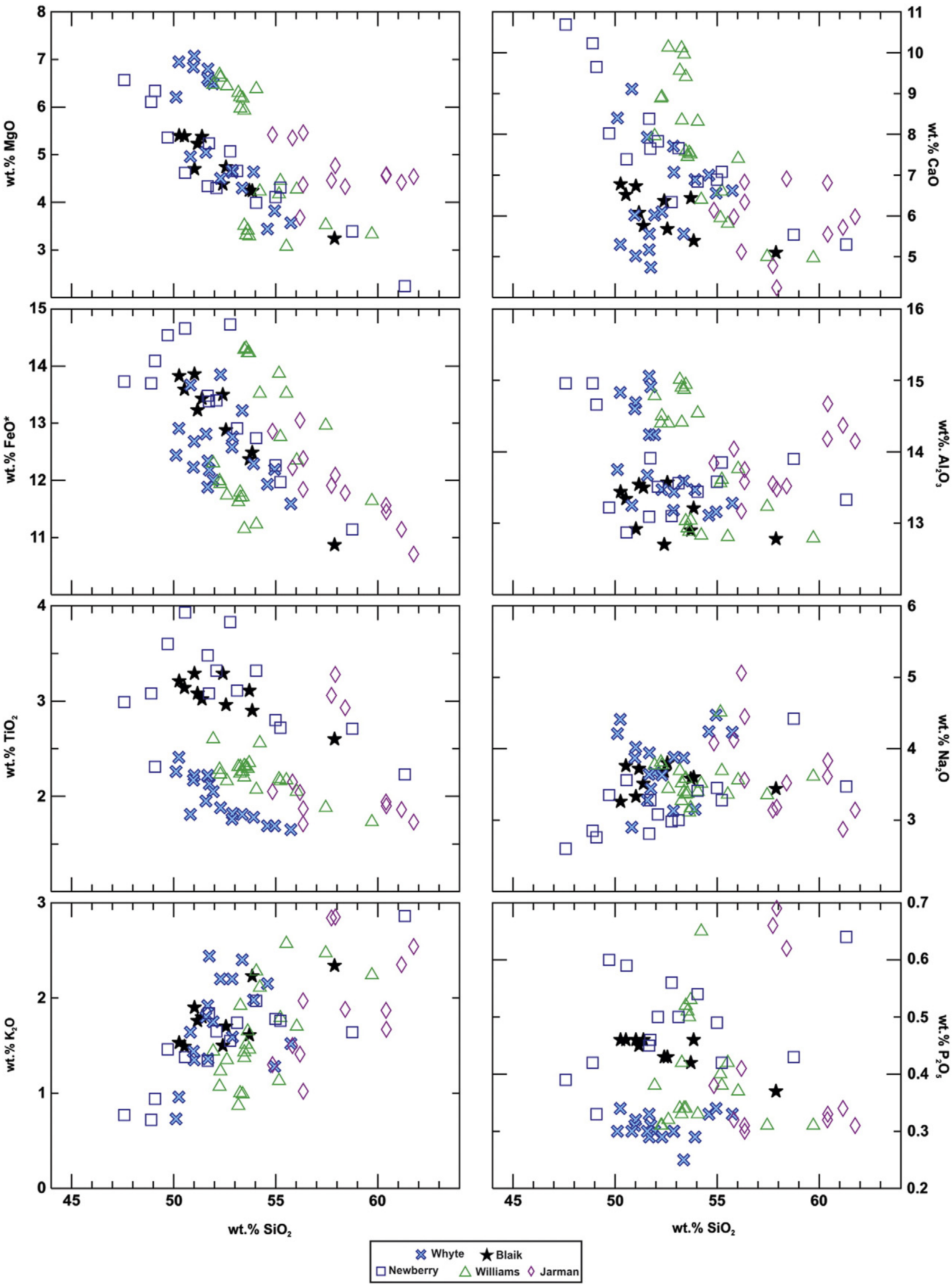

Fig. 6. Harker diagrams illustrating representative major element variations of the well cuttings.

to each other, they encountered the products of numerous eruptive loci (Brueseke et al., 2014; Bulen, 2012; Hobbs, 2015). In this context, Brueseke et al. (2014) suggested that SOA volcanism may have resembled "plains-style" volcanism characterized by eruptions from fissures and shield volcanoes similar to the Cenozoic basalts in the northwestern United States (U.S.A.) from the Snake River plain and

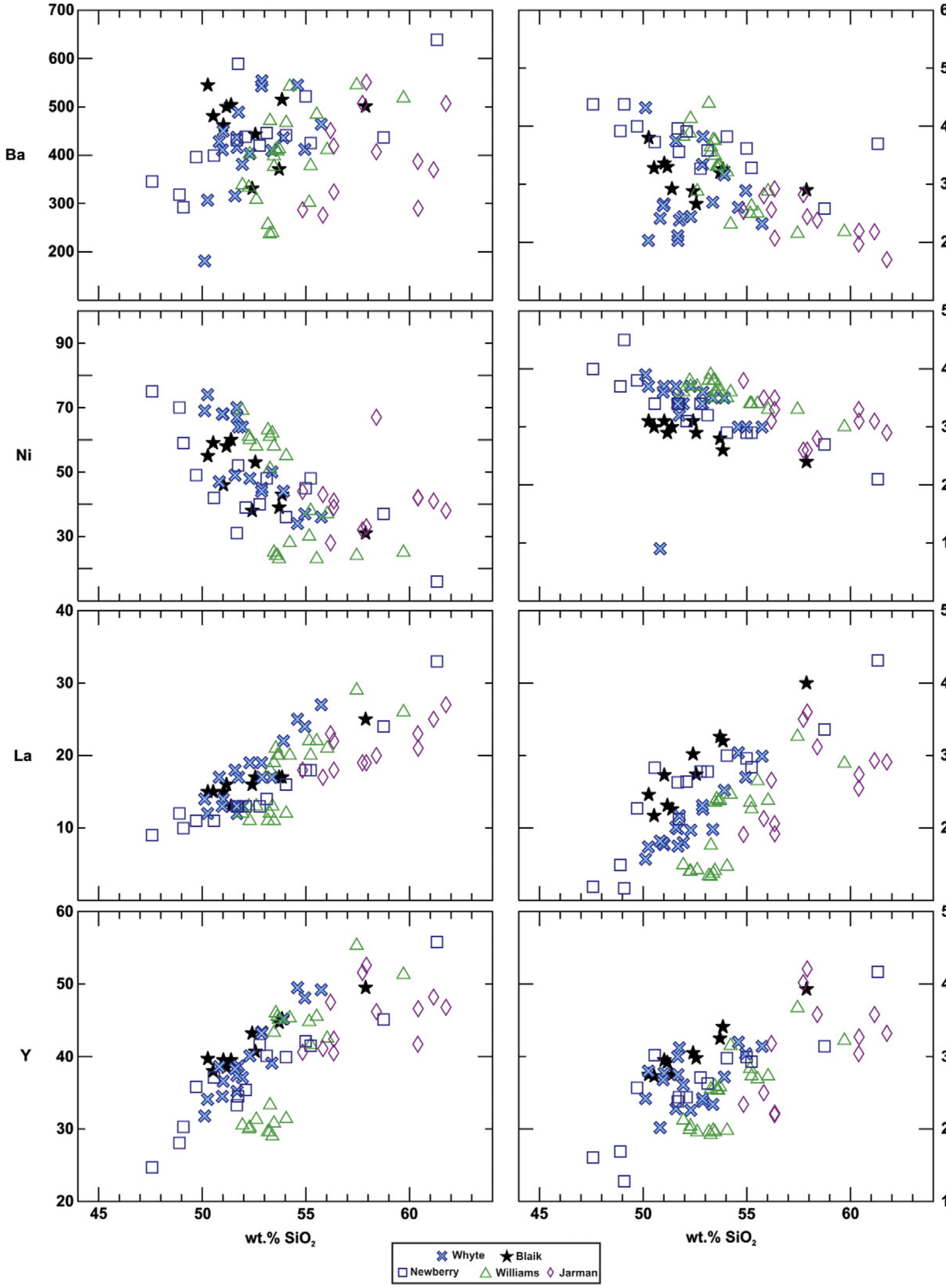

Fig. 7. Harker diagrams illustrating representative trace element variations of the well cuttings.

eastern Oregon (e.g. Bondre and Hart, 2008; Brueseke et al., 2007; Greeley, 1982; Hughes et al., 1999).

3.4. Sr and Nd radiogenic isotopes

Fig. 12 illustrates the age-corrected (to 535 Ma) $^{87}Sr/^{86}Sr_i$ and εNd_i values of five Arbuckle samples with both Sr and Nd isotope results. One sample (CB-PAJ-13) has $^{87}Rb/^{86}Sr = 5.26$, which yields an unrealistic $^{87}Sr/^{86}Sr$ ratio $= 0.66693$; we interpret this to reflect Rb addition and Sr loss, likely due to post-emplacement alteration. Overall, $^{87}Sr/^{86}Sr_i$ values range from 0.70319 to 0.70877 and εNd_i range from $+1.9$ to 4.1. Sample CB-PAN-20 from the Newberry well has the least radiogenic $^{87}Sr/^{86}Sr_i$ value (0.70319) and the highest εNd_i ($+4.1$). The sample suite defines an array that extends to more radiogenic

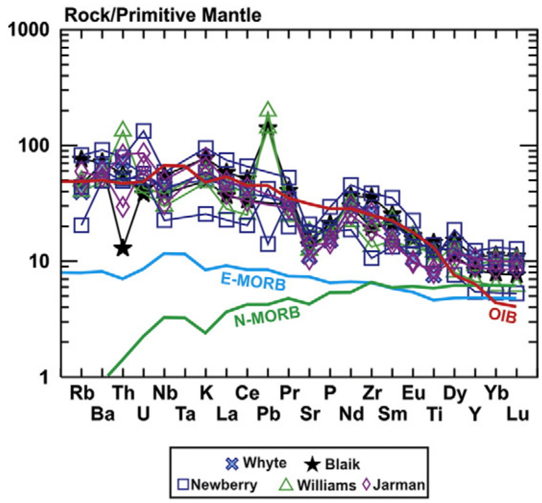

Fig. 8. Primitive mantle normalized trace element variations of the well cuttings modified after Sun and McDonough (1989). OIB, ocean-island basalt; E-MORB, enriched mid-ocean ridge basalt; N-MORB, normal mid-ocean ridge basalt (mantle compositions from Sun and McDonough, 1989).

$^{87}Sr/^{86}Sr_i$ values as εNd_i slightly decreases (Fig. 12). The overall range of εNd_i overlaps with εNd_i from other SOA mafic igneous rocks, including postulated feeder dikes and Wichita Mountain area gabbros (Fig. 12), however the cuttings tend to have more radiogenic $^{87}Sr/^{86}Sr_i$ compositions. The samples also have similar Nd isotope compositions from other flood basalt provinces (Fig. 12).

4. Discussion

4.1. Geochemical constraints and relationship to other Cambrian mafic rocks of the SOA

The bulk chemistry and isotope characteristics of the cuttings overlap with worldwide continental flood basalts/OIBs (Figs. 8, 9, 12). On the tectonic discrimination diagram of Meschede (1986), the samples plot as intraplate tholeiitic basalts (Fig. 13). They also plot in the "within plate" field of Pearce and Norry (1979), based on their Zr and Y concentrations. Other discrimination diagrams (Mullen, 1983; Pearce and Cann, 1973) classify the samples in a similar way (Bulen, 2012; Hobbs,

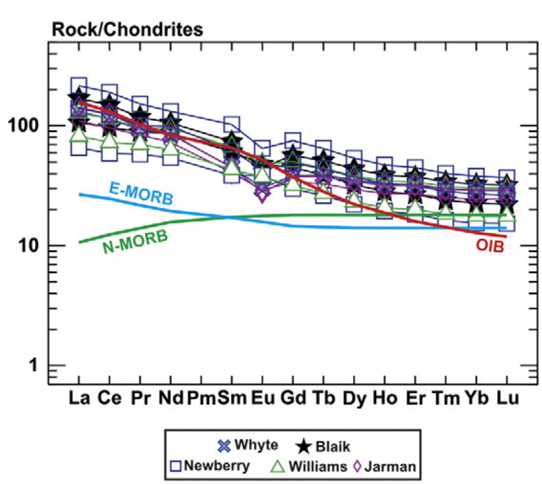

Fig. 9. Well cutting rare earth element compositions normalized to chondrite (after Sun and McDonough (1989). OIB, ocean-island basalt; E-MORB, enriched mid-ocean ridge basalt; N-MORB, normal mid-ocean ridge basalt (mantle compositions from Sun and McDonough, 1989).

2015). These results are consistent with intraplate mafic volcanism and, coupled with the existing geophysical and stratigraphic constraints, LIP formation. εNd for Arbuckle-area Mesoproterozoic granitoids average + 3.6 (Rohs and Van Schmus, 2007) but there are no published $^{87}Sr/^{86}Sr$ ratios for these rocks, thus making detailed comparison with our samples impossible. The εNd values of these granitoids overlap with our least evolved samples, but εNd does generally decrease with increasing wt.% SiO_2 (Table 1). Also, the sample with the most radiogenic Sr isotope value (CB-PAJ-10) does not have the lowest εNd, indicating that something other than simple crustal interaction accounts for the isotope values of some of these samples. Furthermore, $^{87}Sr/^{86}Sr_i$ ratios increase with decreasing Ba/Nb and Ba/Th, opposite to the relation expected for $^{87}Sr/^{86}Sr$ if the variation were solely due to contamination by upper continental crust. As a result, it is likely that some of the more radiogenic $^{87}Sr/^{86}Sr_i$ ratios may reflect post-magmatic alteration (e.g., fluids, low-T metamorphism) that did not substantially affect the Nd isotope ratios (e.g. Cousens et al., 1993; Halliday et al., 1984). It is our interpretation that sample CB-PAN-20 represents the best view into the dominant mantle source of these cuttings. This sample is a tholeiitic basalt, with relatively high wt.% MgO and low SiO_2 (for this sample suite), has $^{87}Sr/^{86}Sr_i = 0.70319$, and $\varepsilon Nd_i = 4.1$.

Mafic dikes locally cross-cut Precambrian granitoid and gneiss northeast of the study area in the Mill Creek quarry (Lidiak et al., 2014). These dikes have SiO_2 values lower than 52 wt.%, and MgO values between 4.3 and 7.3 wt.%; overall, they are less evolved than the well cuttings. La/Nb values for these samples are between 0.9 and 1.1, staying within the accepted EMI values (Weaver, 1991), and at the higher end of the other Arbuckle values (Lidiak et al., 2014). The Mill Creek dikes have age corrected (to 535 ma) $^{87}Sr/^{86}Sr$ values of 0.70392 to 0.70436 and εNd = 2 to 5.1 (Fig. 14; Lidiak et al., 2014). Lidiak et al. (2014) suggest that the dikes have experienced minor (if any) crustal interaction, thus their trace element and isotope characteristics reflect their mantle source that is interpreted to reflect primarily both depleted and OIB-type mantle components (Lidiak et al., 2014). We suggest these same components are present in the samples from this study, especially CB-PAN-20 (Jarman), the least radiogenic sample reported.

Farther west in the Wichita Mountains (Fig. 2), the Glen Mountain Layered Complex and the Roosevelt Gabbros record Cambrian mafic magmatism. Published data for these units are scarce, however some geochemical data from the Roosevelt Gabbros can be compared to the well cuttings from this study (Gilbert and Hughes, 1986; Shapiro, 1981). Roosevelt Gabbro outcrops are present throughout the Wichita Mountains and give a glimpse into the intrusive component of the magmatism that produced the lavas associated with the proposed flood basalt event in this study (Hanson et al., 2013). The Roosevelt Gabbros show similar geochemical trends to the well cuttings from the Arbuckle Mountains (Fig. 14), although the Roosevelt Gabbros tend to be more primitive, with generally higher wt.% MgO and lower wt.% K_2O. Zr/Nb values are >7 and overlap with some of the cuttings at <55 wt.% SiO_2; these Zr/Nb values generally resemble EMI OIB (~4–12; Weaver, 1991). Some of the other Arbuckle cuttings have slightly lower Zr/Nb (~6–7; Fig. 12). K/P values, which are <3.5 for basaltic rocks not contaminated by K-rich upper crust (Carlson and Hart, 1987), for the intrusives are generally lower than the well cuttings but do overlap at low K/P and low wt.% SiO_2 (Fig. 14). Sr and Nd isotope ratios from the Glen Mountain Layered Complex provide further insight into the similarities between the Wichita and Arbuckle Mountains within the SOA. The overlap between the Glen Mountains Layered Complex and the least radiogenic well cutting (CB-PAN-20) is evident on Fig. 14. These samples also broadly overlap in Sr and Nd isotope space with regional dikes. As a result, it is likely that the Roosevelt Gabbros, the Arbuckle well cuttings, and the dikes are part of the same magmatic event with a broadly similar mantle source(s), as proposed by Hanson et al. (2013).

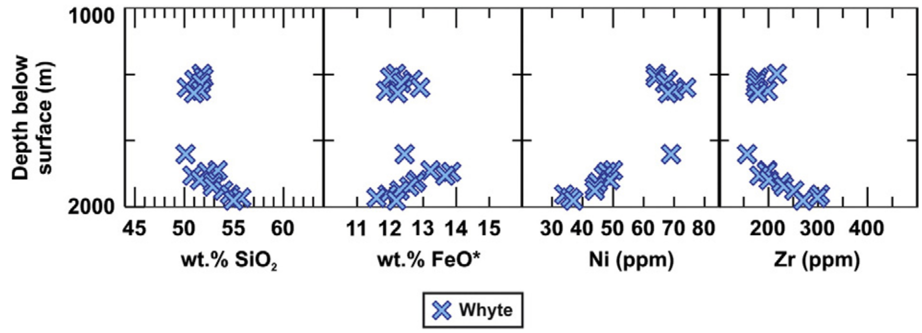

Fig. 10. Chemostratigraphy of Whyte samples; gap between sample clusters consists of primarily rhyolite lavas (Fig. 3).

4.2. Implications for a large igneous province

The inferred eruptive styles of the rocks in this study conform to the definition of flood basalt volcanism discussed by Walker (1993), even though it may be challenging to trace individual lavas across the SOA or constrain the erupted volumes of these lavas because of lack of exposure. This interpretation is supported by the geochemical characteristics of the subsurface mafic-intermediate lavas discussed in this study and prior geophysical work. The cuttings exhibit primarily tholeiitic, intraplate affinities, which are typical of continental rift and flood basalt volcanism (Basaltic Volcanism Study Project, 1981; Hoffman et al., 1974). Volcanism occurring due to a leaky transform fault system, as was suggested by Thomas (2011), is characterized by small-volume alkaline (to transitional) magmatic affinities (Skulski et al., 1991, 1992) and there is no evidence that such eruptive products exist in the SOA. Thus, we suggest that the mafic through intermediate composition rocks in this study were derived from a mantle source consistent with LIP formation and flood basalt volcanism during the formation of the SOA. Subsequent magma evolution processes (e.g., variable amounts of fractional crystallization and crustal interaction) can account for the more evolved compositions of some of the rocks. While more geochronology is needed to better constrain the timing of SOA magmatism, especially the eruptive packages we have studied, it is interesting that the existing ages overlap with the End-Ediacaran extinction event and Cambrian boundary at 541 ± 1.0 Ma (Chen et al., 2014; Cohen et al., 2013; Darroch et al., 2015; Schroder and Grotzinger, 2007; Walker et al., 2013). Recent work suggests that this extinction event occurred due to biological processes (Darroch et al., 2015). However, it might be possible that like other mass extinction events on Earth that have been linked to LIP formation/flood basalt volcanism and associated global environmental change (Jones et al., 2016; Rampino, 2010; Saunders, 2005; Schoene et al., 2015; Self et al., 2014; White and Saunders, 2005), the End-Edicaran event could have also been partially stimulated by SOA magmatism. Continued study of the well cuttings, including more comprehensive radiogenic and stable isotope studies, are needed to decipher the mantle and crustal components of SOA mafic magmatism, to better relate the coeval rhyolites to the mafic-intermediate rocks studied here, and to refine tectonomagmatic models for formation of the SOA.

5. Conclusions

1. Cambrian well cuttings from the Southern Oklahoma Aulacogen are dominantly subalkaline, tholeiitic, basalts to andesites; their primitive mantle normalized trace element compositions resemble ocean island basalts and flood basalts. Overall, $^{87}Sr/^{86}Sr_i$ values from the cuttings range from 0.70319 to 0.70877 and εNd_i range from +1.9 to 4.1. CB-PAN-20 from the Newberry well has the least radiogenic $^{87}Sr/^{86}Sr_i$ value (0.70319) and the highest εNd_i (+4.1).
2. Chemically distinct and stratigraphically controlled samples (e.g., within-well geochemical changes) exist in the subsurface, which are interpreted to represent distinct lava packages. In some cases, these packages appear to record recharge and differentiation events.

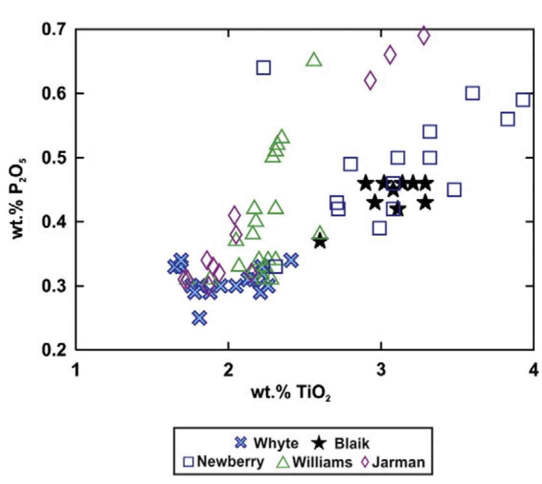

Fig. 11. Wt.% TiO_2 vs. wt.% P_2O_5 for all samples. Notice the overlap between samples from the Blaik and Newberry wells; these samples are from approximately the same stratigraphic depth below the post-volcanic unconformity (Fig. 3).

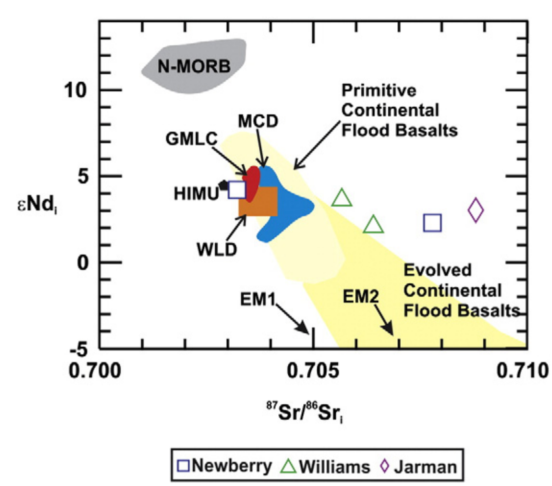

Fig. 12. Initial strontium and neodymium isotopic compositions of well cuttings and mafic igneous rocks of the SOA after Lidiak et al. (2014). $^{87}Sr/^{86}Sr_i$ and εNd_i are calculated at 535 Ma. MCD: Mill Creek quarry dikes (Lidiak et al., 2014); GMLC: Glen Mountain Layered Complex (Lambert et al., 1988); WLD: Wichita late diabase dikes (Hogan et al., 1995, 1996). Flood basalt fields from Condie (2001) while mantle source compositions from Hart (1984, 1988 – HIMU, EM1, EM2) and Sun and McDonough (1989 – N-MORB).

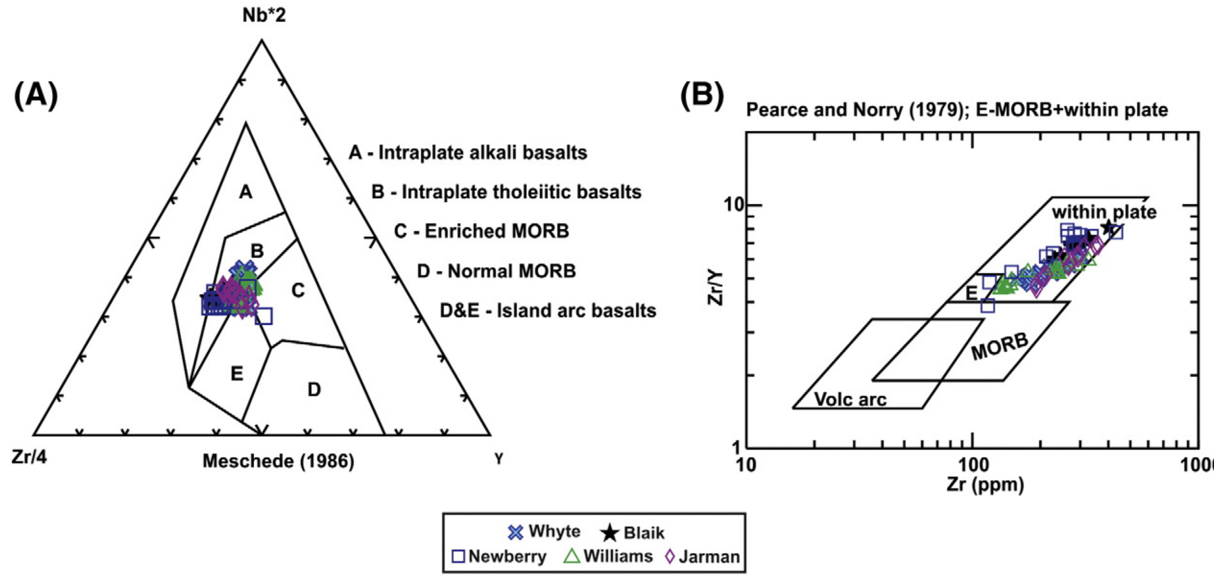

Fig. 13. Tectonic discrimination diagrams after (A) Meschede (1986) and (B) Pearce and Norry (1979); E-MORB; enriched mid-ocean ridge basalt (MORB). Note how the cuttings fall in the same general fields (e.g., intraplate) on both diagrams.

3. The new results presented here, coupled with existing geophysical data and geochemical and isotope data from other mafic rocks in the SOA (e.g., Wichita Mountain area intrusives and subsurface basalts, as well as dikes from the Arbuckle region), and studies of SOA rhyolites, clearly document the presence of an additional flood basalt province in North America where Cambrian SOA magmatism is the outcome of rifting and LIP formation along the southern Laurentian margin.

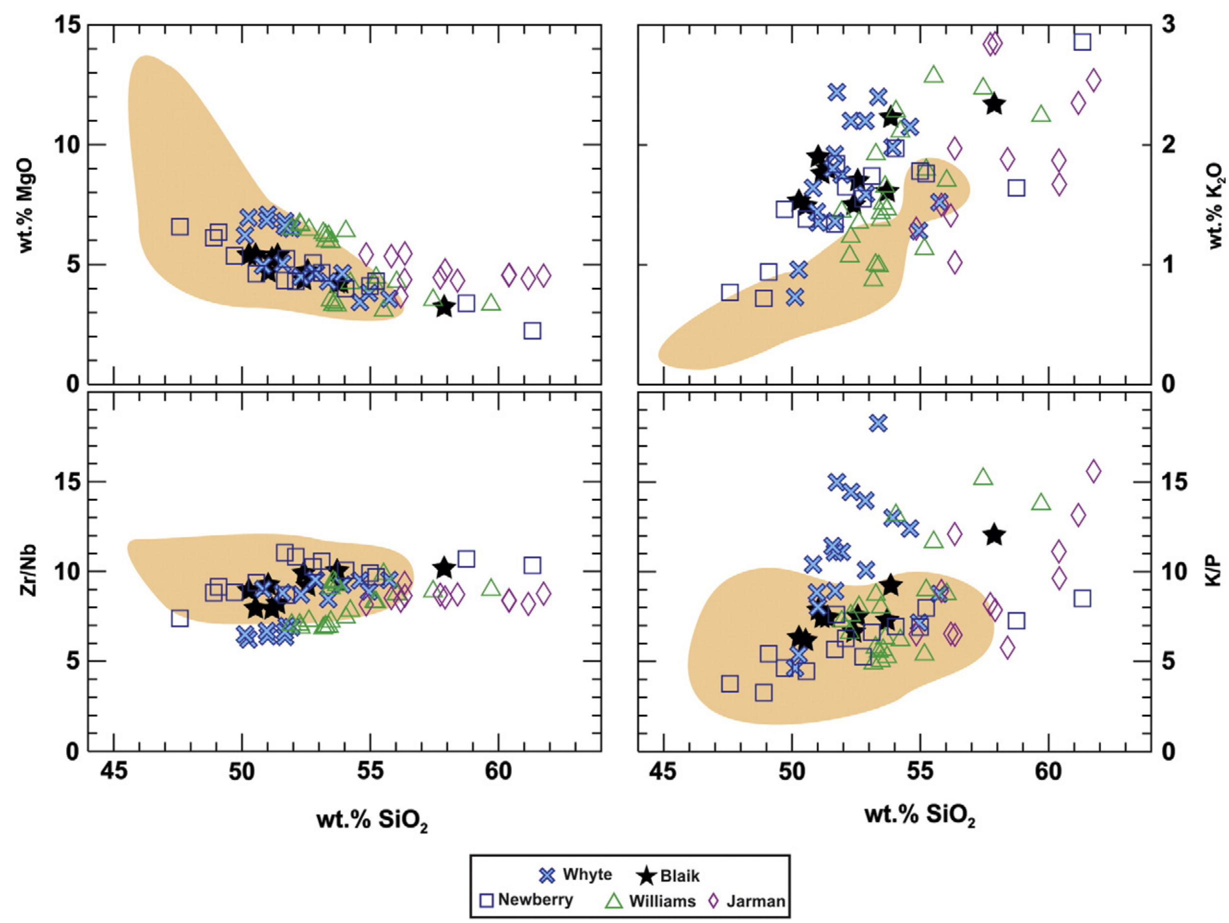

Fig. 14. Wt.% K_2O, wt.% MgO, Zr/Nb ratios, and K/P ratios vs. wt.% SiO_2 for the well cuttings and the Roosevelt Gabbros of the Wichita Mountains (tan field; data from Aquilar, 1988; Gilbert and Hughes, 1986; and Shapiro, 1981). Notice the overlap at low wt.% SiO_2 on all diagrams.

Supplementary data to this article can be found online at http://dx.doi.org/10.1016/j.lithos.2016.05.016.

Acknowledgments

AAPG Grants-in-Aids awarded to Bulen and Hobbs supported this work, as did a KSU-Chapter Sigma Xi Student Research Grant (Hobbs), and funding from the Department of Geology, Kansas State University. National Science Foundation Kansas Louis Stokes Alliance for Minority Participation grant (NSF HRD-1305059) supported Hobbs during this research. Thanks also to Neil Sunenson, and Vyetta Jordan (Oklahoma Geological Survey) for guidance and assistance with this research, to Karen R. Mertzman for all her stellar work in the XRF lab at Franklin and Marshall College, and to John Morton for his superb help with ICP-MS analyses at Miami University. We thank Richard Hanson and Bob Stern for discussions about the well cuttings, Andrea Marzoli, and Robert Trumbull for constructive and positive comments that greatly improved this manuscript, and Andrew Kerr for his comments and editorial handling.

References

Álvaro, J.J., Ezzouhairi, H., Vennin, E., Ribeiero, M.L., Clausen, S., Charif, A., Ait Ayad, N., Moreira, M.E., 2006. The Early-Cambrian Boho volcano of the El Graara massif, Morocco: petrology, geodynamic setting and coeval sedimentation. Journal of African Earth Sciences 44, 396–410.

Aquilar, J., 1988. Geochemistry of Mafic Rock Units of the Southern Oklahoma Aulacogen, Southwestern Oklahoma: University of Oklahoma unpublished M.S. thesis, 167 p.

Arce, J.L., Layer, P.W., Morales-Casique, E., Benowitz, J.A., Rangel, E., Escolero, O., 2013. New constraints on the subsurface geology of the Mexico City Basin: the San Lorenzo Tezonco deep well, on the basis of $^{40}Ar/^{39}Ar$ geochronology and whole-rock chemistry. Journal of Volcanology and Geothermal Research 266, 34–49.

Badger, R.L., Sinha, A.K., 1988. Age and Sr isotopic signature of the Catoctin volcanic province: implications for subcrustal mantle evolution. Geology 16, 692–695.

Badger, R.L., Ashley, K.T., Cousens, B.L., 2010. Stratigraphy and geochemistry of the Catoctin volcanics: implications for mantle evolution during the breakup of Rodinia. In: Tollo, R.P., Bartholomew, M.J., Hibbard, J.P., Karabinos, P.M. (Eds.), From Rodinia to Pangea: The Lithotectonic Record of the Appalachian Region. Geological Society of America Memoir vol. 206, pp. 397–415.

Basaltic Volcanism Study Project, 1981. Basaltic Volcanism on the Terrestrial Planets. Pergamon Press, Inc., New York (1288 p).

Beswick, A.E., Soucie, G., 1978. A correction procedure for metasomatism in an Archean greenstone belt. Precambrian Research 6, 235–248.

Bondre, N.R., Hart, W.K., 2008. Morphological and textural diversity of the Steens Basalt lava flows, Southeastern Oregon, USA: implications for emplacement style and nature of eruptive episodes. Bulletin of Volcanology 70, 999–1019.

Bowring, S.A., Hoppe, W.J., 1982. U–Pb zircon ages from Mount Sheridan Gabbro, Wichita Mountains. In: Gilbert, M.C., Donovan, R.N. (Eds.), Geology of the Eastern Wichita Mountains, Southwestern Oklahoma. Oklahoma Geological Survey Guidebook vol. 21, pp. 54–59.

Branney, M.J., Bonnichsen, B., Andrews, G.D.M., Ellis, B., Barry, T.L., McCurry, M., 2008. 'Snake River (SR)-type' volcanism at the Yellowstone hotspot track: distinctive products from unusual, high-temperature silicic super-eruptions. Bulletin of Volcanology 70, 293–314.

Brueseke, M.E., Heizler, M.T., Hart, W.K., Mertzman, S.A., 2007. Distribution and geochronology of Oregon Plateau (U.S.A.) flood basalt volcanism: the Steens Basalt revisited. Journal of Volcanology and Geochemical Research 161, 187–214.

Brueseke, M.E., Bulen, C.L., Mertzman, S.A., 2014. Major and Trace-Element Constraints on Cambrian Basalt Volcanism in the Southern Oklahoma Aulacogen from Well Cuttings in the Arbuckle Mountains Region, Oklahoma (U.S.a.). In: Suneson, N.H. (Ed.), Oklahoma Geological Survey. Guidebook vol. 38, pp. 95–104.

Bryan, S.E., Ernst, R.E., 2008. Revised definition of large igneous provinces (LIPs). Earth-Science Reviews 86, 175–202. http://dx.doi.org/10.1016/j.earscirev.2007.08.008.

Bryan, S.E., Ferrari, L., 2013. Large igneous provinces and silicic large igneous provinces: progress in our understanding over the last 25 years. Geological Society of America Bulletin 125, 1053–1078. http://dx.doi.org/10.1130/B30820.1.

Bulen, C. L., 2012. The Role of Magmatism in the Evolution of the Cambrian Southern Oklahoma Rift Zone: Geochemical Constraints on the Mafic-Intermediate Rocks in the Arbuckle Mountains, OK. Kansas State University unpublished M.S. thesis, 87 p.

Cameron, M., Weaver, B.L., Diez de Medina, D., 1986. A preliminary report on trace element geochemistry of mafic igneous rocks of the Southern Oklahoma Aulacogen. In: Gilbert, M.C. (Ed.), Petrology of the Cambrian Wichita Mountains Igneous Suite. Oklahoma Geological Survey Guidebook 23, pp. 80–85.

Carlson, R.W., Hart, W.K., 1987. Crustal genesis on the Oregon plateau. Journal of Geophysical Research 92, 6191–6206.

Chen, D., Zhou, X., Fu, Y., Wang, J., Yan, D., 2014. New U—Pb zircon ages of the Ediacaran–Cambrian boundary strata in South China. Terra Nova 27, 62–68.

Cohen, K.M., Finney, S.C., Gibbard, P.L., Fan, J.-X., 2013. The ICS International Chronostratigraphic Chart. Episodes 36, 199–204.

Condie, K.C., 2001. Mantle Plumes and Their Record in Earth History. Cambridge University Press (306 p).

Cousens, B.L., Spera, F.J., Dobson, P.F., 1993. Post-eruptive alteration of silicic ignimbrites and lavas, Gran Canaria, Canary islands: strontium, neodymium, lead, and oxygen isotope evidence. Geochemica et Cosmochimica Acta 57, 631–640.

Dalziel, I.W.D., 2014. Cambrian transgression and radiation linked to an Iaepetus–Pacific oceanic connection? Geology 42, 979–982.

Darroch, S.A.F., Sperling, E.A., Boag, T.H., Raciot, R.A., Mason, S.J., Morgan, A.S., Tweedt, S., Myrow, P., Johnston, D.Y., Erwin, D.H., Laflamme, M., 2015. Biotic replacement and mass extinction of the Ediacara biota. Proceedings of the Royal Society B 282, 20151003.

Degeller, M., Wright, J.E., Hogan, J.P., Gilbert, M.C., Price, J.D., 1996. Age and source characteristics of the Mount Scott Granite, Oklahoma. Geological Society of America Abstracts with Programs 28, 10.

Ernst, R.E., Bleeker, W., 2010. Large igneous provinces (LIPs), giant dyke swarms, and mantle plumes: significance for breakup events within Canada and adjacent regions from 2.5 Ga to present. Canadian Journal of Earth Sciences 47, 695–739.

Eschberger, A.M., Hanson, R.E., Puckett, R.E., 2014. Carlton Rhyolite Group and Diabase Intrusions in the East Timbered Hills, Arbuckle Mountains. In: Suneson, N.H. (Ed.), Oklahoma Geological Survey. Guidebook vol. 38, pp. 143–186.

Gilbert, M.C., Hughes, S.S., 1986. Partial chemical characterization of Cambrian basaltic liquids of the Southern Oklahoma Aulacogen. In: Gilbert, M.C. (Ed.), Petrology of the Cambrian Wichita Mountains Igneous Suite. Oklahoma Geological Survey Guidebook 23, pp. 73–79.

Golonka, J., 2012. Paleozoic Paleoenvironment and Paleolithofacies Maps of Gondwana. Wydawnictwa AGH Publishing House, Kraków (82p).

Golonka, J., Gaweda, A., 2012. Plate tectonic evolution of the southern margin of Laurussa in the Paleozoic. In: Sharkov, E. (Ed.)Tectonics-Recent Advances http://dx.doi.org/10.5772/50009.

Greeley, R., 1982. The Snake River Plain, Idaho: representative of a new category of volcanism. Journal of Geophysical Research 87, 2705–2712.

Green, J.C., Fitz III, T.J., 1993. Extensive felsic lavas and rheoignimbrites in the Keweenawan Micontinent Rift plateau volcanics, Minnesota: petrographic and field recognition. Journal of Volcanology and Geothermal Research 54, 177–196.

Halliday, A.N., Fallick, A.E., Hutchinson, J., Hildreth, W.A., 1984. Nd, Sr, and O isotopic investigation into the causes of chemical and isotopic zonation in the Bishop tuff, California. Earth and Planetary Science Letters 68, 379–391.

Ham, W.E., Denison, R.E., Merritt, C.A., 1964. Basement rocks and structural evolution of southern Oklahoma. Oklahoma Geological Survey Bulletin 95, 160.

Hames, W.E., Hogan, J.P., Gilbert, M.C., 1998. Revised granite–gabbro age relationships, Southern Oklahoma Aulacogen, U.S.A. In: Hogan, J.P., Gilbert, M.C. (Eds.), Basement TectonicsProceedings of the Twelfth International Conference on Basement Tectonics 12. Kluwer, Dordrecht, The Netherlands, pp. 247–249.

Hanson, R.E., Al-Shaieb, Z., 1980. Voluminous subalkaline silicic magmas related to intracontinental rifting in the southern Oklahoma aulacogen. Geology 8, 180–184.

Hanson, R.E., Eschberger, A.M., 2014. An overview of the Carlton Rhyolite Group: Cambrian A-type felsic volcanism in the Southern Oklahoma Aulacogen. In: Suneson, N.H. (Ed.), Oklahoma Geological Survey. Guidebook vol. 38, pp. 123–142.

Hanson, R.E., McCleery, D.A., Crowley, J.L., Bowring, S.A., Burkholder, B.K., Finegan, S.A., Philips, C.M., Pollard, J.B., 2009. Large-scale Cambrian rhyolitic volcanism in southern Oklahoma related to the opening of Iapetus. Geological Society of America Abstracts with Programs 41, 14.

Hanson, R.E., Puckett Jr., R.E., Keller, G.R., Brueseke, M.E., Bulen, C.L., Mertzman, S.A., Finegan, S.A., McCleery, D.A., 2013. Intraplate magmatism related to opening of the southern Iapetus Ocean: Cambrian Wichita igneous province in the Southern Oklahoma rift zone. Lithos 174, 57–70.

Hanson, R.E., Burkholder, B.K., Donovon, R.N., Dart, J.C., Frazier, S.J., McCleery, D.A., Phillips, C.M., Pollard, J.B., 2014. Physical volcanology and geochemistry of the Carlton Rhyolite in the Slick Hills, Wichita Mountains. In: Suneson, N.H. (Ed.), Oklahoma Geological Survey. Guidebook vol. 38, pp. 255–298.

Hart, S.R., 1984. A large-scale isotope anomaly in the Southern Hemisphere mantle. Nature 309, 753–757.

Hart, S.R., 1988. Heterogeneous mantle domains: signatures, genesis, and mixing chronologies. Earth and Planetary Science Letters 90, 273–296.

Hobbs, J., 2015. Petrologic Constraints of Cambrian Mafic to Intermediate Volcanism in the Southern Oklahoma Aulacogen. Kansas State University unpublished M.S. thesis, 76 p.

Hoffman, P., Dewey, J.F., Burke, K., 1974. Aulacogens and their genetic relation to geosynclines, with a Proterozoic example from Great Slave Lake, Canada. In: Dott Jr., R.H., Shaver, R.H. (Eds.), Modern and ancient geosynclinal sedimentation. SEPM Special Publication 19, pp. 38–55.

Hogan, J.P., Amato, J.M., 2015. Confirmation of temporally distinct magmatic events in the Wichita Mountains, Oklahoma Presented at the Geological Society of America South Central Section Meeting 47, p. 13.

Hogan, J.P., Gilbert, M.C., Price, J.D., Wright, J.E., 1995. Petrogenesis of A-type sheet-granites from an ancient rift. In: Brown, M., Piccoli, P.M. (Eds.), The Origin of Granites and Related Rocks: Third Hutton Symposium Abstracts. U.S. Geological Survey Circular 1129, pp. 68–69.

Hogan, J.P., Gilbert, M.C., Price, J.D., Wright, J.E., Hames, W.E., 1996. Magmatic evolution of the southern Oklahoma aulacogen. Geological Society of America Abstracts with Programs 28, 19.

Hooper, P.R., 2000. Chemical discrimination of Columbia River basalt flows. Geochemistry, Geophysics, Geosystems 1. http://dx.doi.org/10.1029/2000GC000040.

Hughes, S.S., Smith, R.P., Hackett, W.R., Anderson, S.R., 1999. Mafic volcanism and environmental geology of the Eastern Snake River Plain, Idaho. In: Hughes, S.S., Thackray, G.D. (Eds.), Guidebook to the Geology of Eastern Idaho: Idaho Museum of Natural History, pp. 143–168.

Jones, M.T., Jerram, D.A., Svensen, H.H., Grove, C., 2016. The effects of large igneous provinces on global carbon and Sulphur cycles. Paleogeography, Paleoclimatology, Paleoecology 441, 4–21.

Keller, G.R., Stephenson, R.A., 2007. The Southern Oklahoma and Dniepr-Donets aulacogens: a comparative analysis. In: Hatcher Jr., R.D., Carlson, M.P., McBride, J.H., Martinez Catalan, J.R. (Eds.), 4-D Framework of Continental Crust. Geological Society of America Memoir 200, pp. 127–143.

Krogh, T.E., 1982. Improved accuracy of U—Pb ages by the creation of more concordant systems using an air abrasion technique. Geochimica et Cosmochimica Acta 46, 637–649.

Lambert, D.D., Unruh, D.M., Gilbert, M.C., 1988. Rb—Sr and Sm—Nd isotopic study of the Glen Mountains Layered Complex: initiation of rifting within the Southern Oklahoma aulacogen. Geology 16, 13–17.

LeBas, M.J., Le Maitre, R.W., Streckeiser, A., Zanettin, B., 1986. Chemical classification of volcanic rocks based on total alkali-silica diagram. Journal of Petrology 27, 745–750.

LeMaitre, R.W., 1976. The chemical variability of some common igneous rocks. Journal of Petrology 17, 589–637.

Lidiak, E.G., Denison, R.E., Stern, R.J., 2014. Cambrian (?) Mill Creek Diabase Dike Swarm, Eastern Arbuckles: a glimpse of Cambrian rifting in the Southern Oklahoma Aulacogen. In: Suneson, N.H. (Ed.), Oklahoma Geological Survey. Guidebook vol. 38, pp. 105–122.

Manley, C.R., 1996. In situ formation of welded tuff-like textures in the carapace of a voluminous silicic lava flow, Owyhee County, SW Idaho. Bulletin of Volcanology 57, 672–686.

McClellan, E., Gazel, E., 2014. The Cryogenian intra-continental rifting of Rodinia: evidence from the Laurentian margin in eastern North America. Lithos 206-207, 321–337.

McConnell, D.A., Gilbert, M.C., 1990. Cambrian extensional tectonics and magmatism within the Southern Oklahoma Aulacogen. In: Lucchitta, I., Morgan, P. (Eds.), Heat and Detachment in Continental Extension. Tectonophysics 174, pp. 147–157.

Mertzman, S.A., 2000. K—Ar results from the southern Oregon–northern California Cascade Range. Oregon Geology 62, 99–122.

Mertzman, S.A., 2015. XRF laboratory: overview and analytical procedures. http://www.fandm.edu/earth-environment/laboratory-facilities/instrument-use-and-instructions (Accessed 1/12/2016).

Meschede, M., 1986. A method of discriminating between different types of mid-ocean ridge basalts and continental tholeiites with the Nb—Zr—Y diagram. Chemical Geology 56, 207–218.

Milner, S.C., Duncan, A.R., Ewart, A., 1992. Quartz latite rheoignimbrites flows of the Etendeka Formation, north-western Namibia. Bulletin of Volcanology 54, 200–219.

Mullen, E.D., 1983. $MnO/TiO_2/P_2O_5$: a minor element discriminant for basaltic rocks of oceanic environments and its implications for petrogenesis. Earth and Planetary Science Letters 62, 53–62.

Patchett, P.J., Ruiz, J., 1987. Nd isotopic ages of crust formation and metamorphism in the Precambrian of eastern and southern Mexico. Contributions to Mineralogy and Petrology 96, 523–528.

Pearce, J.A., Cann, J.R., 1973. Tectonic setting of basic volcanic rocks determined using trace element analyses. Earth and Planetary Science Letters 19, 290–300.

Pearce, J.A., Norry, M.J., 1979. Petrogenetic implications of Ti, Zr, Y, and Nb variations in volcanic rocks. Contributions to Mineralogy and Petrology 69, 33–47.

Pouclet, A., Ouazzani, H., Fekkak, A., 2008. The Cambrian volcano-sedimentary formations of westernmost High Atlas (Morocco): their place in the geodynamic evolution of the West African Palaeo-Gondwana northern margin. In: Ennih, N., Liégeois, J.-P. (Eds.), The Boundaries of the West African Craton. Geological Society, London, Special Publications vol. 297, pp. 303–327.

Puckett, R.E., 2011. A thick sequence of rift-related basalts in the Arbuckle Mountains, Oklahoma, as revealed by deep drilling. Shale Shaker 2011, 207–216 (Jan/Feb).

Puckett, R.E., Hanson, R.E., Eschberger, A.M., Brueseke, M.E., Bulen, C.L., Price, J.D., 2014. New insight into the Early Cambrian igneous and sedimentary history of the Arbuckle Mountains Area of the Southern Oklahoma Aulacogen from basement well penetration. In: Suneson, N.H. (Ed.), Oklahoma Geological Survey. Guidebook vol. 38, pp. 61–94.

Puffer, J.H., 2002. A Late Neoproterozoic eastern Laurentian superplume: location, size, chemical composition, and environmental impact. American Journal of Science 302, 1–27.

Rampino, M.R., 2010. Mass extinctions of life and catastrophic flood basalt volcanism. Proceedings of the National Academy of Sciences 107, 6555–6556.

Rohs, C.R., Van Schmus, W.R., 2007. Isotopic connections between basement rocks exposed in the St. Francois Mountains and the Arbuckle Mountains, southern midcontinent, North America. International Journal of Earth Sciences 96, 599–611.

Saunders, A.D., 2005. Large igneous provinces: origin and environmental consequences. Elements 1, 259–263.

Schoene, B., Samperton, K.M., Eddy, M.P., Keller, G., Adatte, T., Bowring, S.A., Khadri, S.F.R., Gertsch, B., 2015. U—Pb geochronology of the Deccan Traps and relation to the end Cretaceous mass extinction. Science 347, 182–184.

Schroder, S., Grotzinger, J.P., 2007. Evidence for anoxia at the Ediacaran–Cambrian boundary: the record of redox-sensitive trace elements and rare earth elements in Oman. Journal of the Geological Society 164, 175–187.

Scotese, C.R., 2009. Late Proterozoic plate tectonics and palaeogeography: a tale of two supercontinents, Rodinia and Pannotia. In: Craig, J., Thurow, J., Thusu, B., Whitham, A., Abutarruna, Y. (Eds.), Global Neoproterozoic Petroleum Systems: The Emerging Potential in North Africa. Geological Society of London Special Publications 326, pp. 67–83.

Self, S., Schmidt, A., Mather, T.A., 2014. Emplacement characteristics, time scales, and volcanic gas release rates of continental flood basalt eruptions on Earth. In: Keller, G., Kerr, A.C. (Eds.), Volcanism, Impacts, and Mass Extinctions: Causes and Effects. Geological Society of America Special Paper vol. 505, pp. 319–337.

Shapiro, B.E., 1981. Chemistry and Petrography of the Navajoe Mountain Basalt Spillites of Southern Oklahoma: University of Texas at Arlington unpublished M.S. thesis, (116 p).

Shervais, J.W., Vetter, S.K., Hanan, B.B., 2006. Layered mafic sill complex beneath the eastern Snake River Plain: evidence from cyclic geochemical variations in basalt. Geology 34, 365–368.

Sheth, H., Cañón-Tapia, E., 2014. Are flood basalt eruptions monogenetic or polygenetic? International Journal of Earth Science 104, 2147–2162.

Skulski, T., Francis, D., Ludden, J., 1991. Arc-transform magmatism in the Wrangell volcanic belt. Geology 19, 11–14.

Skulski, T., Francis, D., Ludden, J., 1992. Volcanism in an arc-transform transition zone: the stratigraphy of the Saint Clare Creek volcanic field, Wrangell volcanic belt, Yukon, Canada. Canadian Journal of Earth Science 29, 446–461.

Sun, S.S., McDonough, W.F., 1989. Chemical and isotopic systematics of oceanic basalts: implications for mantle composition and processes. Geological Society, London, Special Publications 42, 313–345.

Thomas, W.A., 2006. Tectonic inheritance at a continental margin. GSA Today 16, 4–11.

Thomas, W.A., 2011. The Iapetan rifted margin of southern Laurentia. Geosphere 7, 97–120.

Thomas, W.A., 2014. The Southern Oklahoma Transform-Parallel Intracratonic Fault System. In: Suneson, N.H. (Ed.), Oklahoma Geological Survey. Guidebook vol. 38, pp. 375–388.

Thomas, W.A., Astini, R.A., 1996. The Argentine Precordillera: a traveler from the Ouachita Embayment of North American Laurentia. Science 273, 752–757.

Thomas, W.A., Tucker, R.D., Astini, R.A., Denison, R.E., 2012. Ages of pre-rift basement and synrift rocks along the conjugate rift and transform margins of the Argentine Precordillera and Laurentia. Geosphere 8, 1–18.

Thompson, R.N., Morrison, M.A., Dickin, A.P., Hendry, G.L., 1983. Continental flood basalts…Arachnids rule OK? In: Hawkesworth, C.J., Norry, M.J. (Eds.), Continental Basalts and Mantle Xenoliths: Shiva, pp. 158–185

Toews, C.E., Hanson, R.E., Boro, J.R., Eschberger, A.M., 2015. Cambrian basaltic vent conduits in the West Timbered Hills, Arbuckle Mountains, southern Oklahoma: evidence for explosive phreatomagmatic eruptions during rift-related volcanism. Geological Society of America Abstracts with Programs 47, 810.

Walker, G.P., 1993. Basaltic-volcano systems. Geological Society, London, Special Publications 76, 3–38.

Walker, J.D., Geissman, J.W., Bowring, S.A., Babcock, L.E., 2013. The Geological Society of America Geologic Time Scale. Geological Society of America Bulletin 125, 259–272.

Weaver, B.L., 1991. The origin of ocean island basalt end-member compositions: trace element and isotopic constraints. Earth and Planetary Science Letters 104, 381–397.

White, R.V., Saunders, A.D., 2005. Volcanism, impact and mass extinctions: incredible or credible coincidences? Lithos 79, 299–316.

Winchester, T.A., Floyd, P.A., 1977. Geochemical discrimination of different magma series and their differentiation products using immobile elements. Chemical Geology 20, 325–343.

Wright, J.E., Hogan, J.P., Gilbert, M.C., 1996. The Southern Oklahoma Aulacogen: not just another B.L.I.P. American Geophysical Union Transactions 80, F845.

Youbi, N., 19 others, 2011. The Central Iapetus Magmatic Province (CIMP) Large Igneous Province. Distribution, nature, origin, and environmental impact. AAPG Search and Discovery, Article #90137.